

1 Exploring the role of hydrological pathways in modulating multi-annual climate teleconnection
2 periodicities from UK rainfall to streamflow.

3 William Rust ^a; Mark Cuthbert ^b; John Bloomfield ^c; Ron Corstanje ^d; Nicholas Howden ^e; Ian Holman ^a

4 a Cranfield Water Science Institute (CWSI), Cranfield University, Bedford MK43 0AL

5 b School of Earth and Ocean Sciences, Cardiff University, Park Place, Cardiff, CF10 3AT

6 c British Geological Survey, Wallingford, OX10 8ED

7 d Centre for Environment and Agricultural Informatics, Cranfield University, Bedford MK43 0AL

8 e School of Civil, Aerospace and Mechanical Engineering, Queen's Building, University Walk,
9 Clifton BS8 1TR

10

11 Correspondence to William Rust (w.d.rust@cranfield.ac.uk)

12 Abstract

13 An understanding of multi-annual behaviour in streamflow allows for better estimation of the
14 risks associated with hydrological extremes. This can enable improved preparedness for
15 streamflow-dependant services such as freshwater ecology, drinking water supply and
16 agriculture. Recently, efforts have focused on detecting relationships between long-term
17 hydrological behaviour and oscillatory climate systems (such as the NAO). For instance, the
18 approximate 7-year periodicity of the NAO has been detected in groundwater level records in
19 the North Atlantic region, providing potential improvements to the preparedness for future
20 water resource extremes due to their repeating, periodic nature. However, the extent to which
21 these 7-year NAO-like signals are propagated to streamflow, and the catchment processes
22 that modulate this propagation, are currently unknown. Here, we show statistically significant
23 evidence that these 7-year periodicities are present in streamflow (and associated catchment
24 rainfall), by applying multi-resolution analysis to a large dataset of streamflow and associated
25 catchment rainfall across the UK. Our results provide new evidence for spatial patterns of NAO
26 periodicities in UK rainfall with areas of greatest NAO signal found in south west England,
27 South Wales, Northern Ireland and central Scotland, and that NAO-like periodicities account
28 for a greater proportion of streamflow variability in these areas. Furthermore, we find that
29 catchments with greater subsurface pathway contribution, as characterised by the Baseflow
30 Index (BFI), generally show increased NAO-like signal strength; and that subsurface response
31 times (as characterised by Groundwater response Time (GRT)) of between 4 and 8 years,

32 show a greater signal presence still. Our results provide a foundation of understanding for the
33 screening and use of streamflow teleconnections for the improving the practice and policy of
34 long-term streamflow resource management.

35

36 1. Introduction

37 Meteorological conditions in many parts of the world are modulated by large-scale ocean-
38 atmosphere systems, such as the Pacific Decadal Oscillation (PDO) and El Niño Southern
39 Oscillation (ENSO) in the western US (DeFlorio et al, 2013); and the North Atlantic Oscillation
40 (NAO) in Europe (Trigo et al, 2002; Hurrell and Van Loon; 1997), with important multi-annual
41 periodicities (Labat, 2010; Kuss and Gurdak; 2014). The NAO, a dipolar system of
42 atmospheric pressure in the North Atlantic region (Hurrell and Deser, 2010), has been shown
43 to account for the majority of European rainfall variability during the winter months, and is
44 particularly influential in western Europe (West et al., 2019, Uvo, 2003; Alexander et al., 2005;
45 López-Moreno et al., 2011). This is achieved through a modulation of westerly storm tracks
46 (Trigo et al., 2002; Dawson et al., 2004) and Gulf Stream strength (Frankignoul et al., 2001;
47 Chaudhuri et al., 2011; Watelet et al., 2017) by the winter state of the NAO. As such, the NAO
48 has been shown to drive hydrological variability in Europe including river flow (Kingston et al.,
49 2011; Svensson et al. 2015) and groundwater systems (Rust et al., 2019, Neves et al., 2019;
50 Holman et al, 2011).

51

52 In addition to sub-annual variability, the NAO has been shown to exhibit a weak multi-annual
53 cycle of between 6 and 9 years, often described as pseudo-periodic due to its varying strength
54 (Hurrell et al., 2003; Zhang et al., 2011; Olsen and Knudsen, 2012). Despite this reported
55 weakness, many hydro-climatology studies have identified a relationship between the NAO
56 index (NAOI) and groundwater level records, at multi-annual frequencies, in the USA (e.g
57 Kuss and Gurdak, 2014), continental Europe (e.g. Neves et al., 2019) and the UK (e.g. Holman

58 et al., 2011). The strength of these detected cycles in groundwater records is often
59 considerably stronger than those found in the NAOI, indicating that the 6- to 9-year periodicity
60 of the NAO may still yield a considerable modulation on hydrological systems that are sensitive
61 to long-term changes in water fluxes, such as groundwater stores. (Bloomfield and Marchant,
62 2013; Forootan et al., 2018; Van Loon, 2015). Rust et al (2019) compared NAO-like
63 periodicities in composite rainfall records and groundwater levels in the UK's principal aquifers,
64 demonstrating the degree to which multi-annual periodic signals (similar to those in the NAO)
65 can be modulated through part of the hydrological cycle. Given the presence of these multi-
66 annual cycles in both UK rainfall and groundwater records, it follows that these signals may
67 be propagated to streamflow, particularly in groundwater-dominated streams such as those
68 found in many parts of southern and eastern England (Bloomfield et al., 2009). High baseflow
69 streams are often critical for the function of public water supply, freshwater ecosystems, and
70 provide a greater amenity value for surrounding areas (Acreman and Dunbar, 2004).
71 Therefore, an understanding of the catchment processes that modulate multi-annual cycles in
72 streamflow may provide a new opportunity to better manage the long-term use and
73 sustainability of these streamflow-dependant services (Acreman and Dunbar, 2004; Chun et
74 al., 2009). While existing studies have shown that the winter-averaged NAO can modulate
75 streamflow in the UK at an annual scale (Kingston et al., 2006), the strength and spatiality of
76 multi-annual cycles in streamflow, and the catchment processes that modulate them, have yet
77 to be assessed.

78

79 Hydrological pathways are often used to conceptualise the propagation of effective rainfall
80 signals (rainfall minus evapotranspiration) through a catchment to streamflow (Misumi et al.,
81 2001; Bracken et al., 2013; Crossman et al., 2014; Lane et al., 2019). For example, surface
82 pathways are the result of infiltration- or saturation-excess runoff from the land surface and
83 provide a direct response to rainfall in the order of hours or days (Nathan and McMahon, 1990;
84 Gericke and Smithers, 2014; Kronholm and Capel, 2016). Subsurface pathways (such as the

85 travel of water through the unsaturated zone and groundwater flow paths to channel baseflow)
86 exhibit generally lower celerities than surface pathways and can produce a protracted
87 response to rainfall in the order of months or years where faster subsurface pathways
88 dominate (Carr and Simpson, 2018; Hellwig and Stahl, 2018), but ranging to decades or even
89 millennia for longer, deeper groundwater flow pathways with low hydraulic diffusivity
90 (Rousseau-Gueutin *et al.*, 2013; Cuthbert *et al.*, 2019). Existing research into periodic NAO
91 teleconnections with groundwater resources has highlighted the importance of subsurface
92 pathway responsiveness in modulating NAO-like signals in groundwater stores (Kuss and
93 Gurdak, 2014; Neves *et al.*, 2019; Rust *et al.*, 2019). Where a groundwater resource receives
94 a periodic recharge signal (such as those from a climatic teleconnection), Townley (1995)
95 suggests that pathways with response times shorter than the period length will propagate
96 these signals to baseflow more effectively, with minimal damping. Conversely, groundwater
97 pathways with response times longer than the period length cannot convey these signals to
98 the stream at a sufficient rate, meaning the amplitude of the periodic signal is damped as it
99 passes through the aquifer. Therefore, in the case of streamflow, we may expect that;

- 100 i. the propagation of multi-annual periodic signals from rainfall to streamflow is
101 dependent on the relative contribution of surface and subsurface (e.g.
102 groundwater) hydrological pathways within a catchment.
- 103 ii. response times of subsurface pathways will modulate the amplitude of multi-annual
104 periodic signals in streamflow where they are propagated by subsurface pathways

105 Finally, these effects (modulation of NAO signal propagation by hydrological pathways) may
106 be expected to differ between winter and summer streamflow. Catchments in the UK have
107 been shown to receive the strongest NAO signals in winter rainfall (Alexander *et al.*, 2005;
108 Hurrell and Deser, 2010; West *et al.*, 2019). However, given the degree of fine-scale variability
109 seen in precipitation records (Meinke *et al.*, 2005), winter streamflow may contain a relatively
110 low signal-to-noise ratio as surface (and some subsurface) hydrological pathways respond to
111 rainfall within the same winter season. Conversely, slower subsurface pathways provide a

112 protracted response to winter rainfall signals, and are generally accepted to filter finer-scale
113 variability (Bloomfield and Marchant, 2013). As such, we may expect the NAO teleconnection
114 to have a greater influence on summer streamflow in permeable catchments which have a
115 greater contribution from sub surface pathways (baseflow), and proportionally less
116 contribution from surface pathways. In these instances, we may expect the teleconnection
117 between NAO and UK streamflow may be asymmetric between summer and winter. If multi-
118 annual periodic signals in streamflow are present via a teleconnection with the NAO, their use
119 for improving long-term projection of hydrological extremes will rely on an understanding of
120 the catchment processes that modulate the strength of these signals, and their seasonal
121 sensitivities.

122

123 The aim of this paper is to assess the extent to which NAO-like multi-annual signals are
124 propagated from rainfall to streamflow across the UK, and to assess how this is modulated by
125 the relative contribution of faster and slower hydrological pathways. We define NAO-like as
126 those multi-annual cycles in hydro-meteorological records that cover a wide spatial domain
127 and are similar in length to the 6-9 year periodicity reported in the NAO, which we might expect
128 given the control between the NAO and hydrological systems (Svensson et al, 2015).

129

130 This aim will be met by addressing the following research objectives:

- 131 1. Characterise the strength, statistical significance and spatial distribution of NAO-like
132 multi-annual periodicities in rainfall and associated UK streamflow
- 133 2. Quantify the relationship between catchment pathway contribution and response times
134 and the NAO teleconnection by comparing NAO-like periodicity strength in summer
135 and winter streamflow.

136

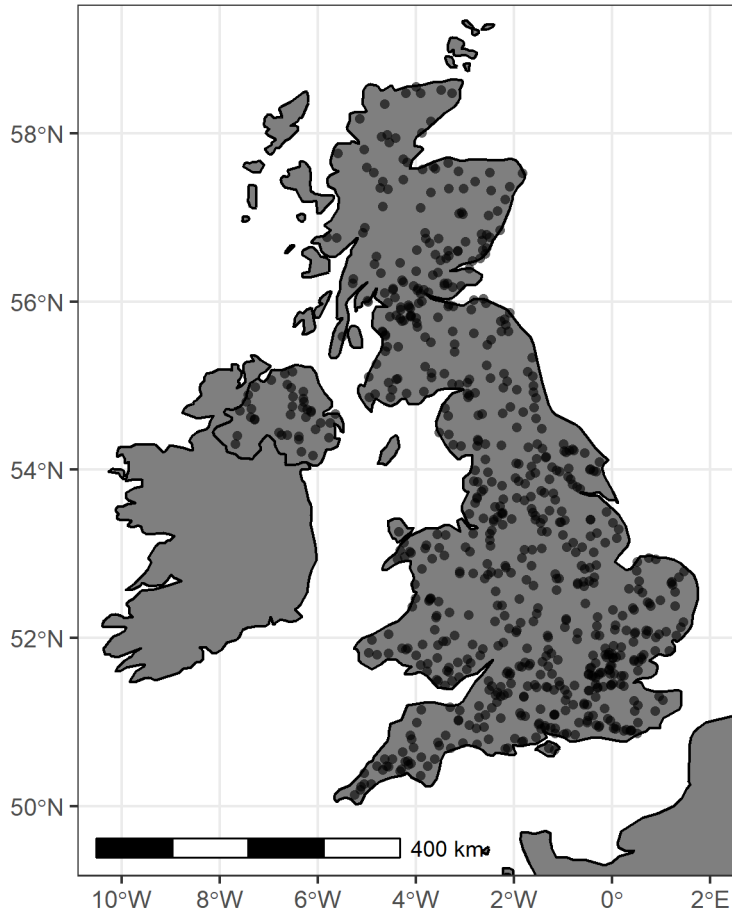
137 2. Data and Methods

138 2.1. Streamflow data

139 Monthly streamflow data and catchment metadata from the UK National River Flow Archive
140 (NRFA; Dixon et al., 2013: <http://nrfa.ceh.ac.uk/>) has been used in this study. Gauging stations
141 with more than 20 years of continuous streamflow data (and coincident catchment rainfall,
142 discussed in the following section), and no data gaps greater than 12 months were initially
143 selected. Where there were multiple gauging stations in a single named river catchment, only
144 the sites with the largest catchment area were taken forward. This produced a final list of 705
145 streamflow gauging stations for use in this study. These streamflow records range from 20 to
146 128 years in length, with a median length of 44.6 years (536 months). These sites provide a
147 representative sample of sites from across the UK, with minimal bias towards the south of
148 England, as indicated by Fig 1. It should be noted that ideally, streamflow that has minimal
149 influence from human factors should be used in hydroclimate studies to avoid confounding
150 mechanisms, however no such large-scale dataset exists for the UK. Furthermore, over the
151 period of analysis and the broad scale of this assessment, inconsistencies in the way water
152 resource management practices are implemented is expected to result in noise to the
153 observations rather than some systematic signal or bias that would affect the results of this
154 paper.

155 2.1. Catchment Rainfall data

156 Calculated monthly rainfall totals for each streamflow gauge catchment are also provided by
157 the NRFA. This dataset has been derived from CEH-GEAR data (Tanguy et al., 2019), which
158 covers the 1890 – 2015 time period, using NRFA catchment boundaries. This catchment
159 rainfall dataset has been used in multiple studies investigating catchment hydrology dynamics
160 and catchment response to rainfall signals (Chiverton et al., 2015; Guillod et al., 2018; Gnann
161 et al., 2019).



162

163 Figure 1 – Locations of streamflow gauges used in this study.

164

165

166 2.2. Catchment Metadata

167 In order to categorise the relative influence of surface and subsurface hydrological pathways

168 on streamflow, the Base Flow Index (BFI) from the NRFA has been used for each streamflow

169 gauge (Gustard et al., 1992). The BFI is a calculated proportion of the flow hydrograph

170 (ranging from 0 to 1) that is derived from slower subsurface pathways such as groundwater-

171 driven baseflow, where 1 is entirely baseflow. While empirical, BFI has been shown to be

172 effective in relating physical catchment pathway processes to streamflow behaviour

173 (Bloomfield et al., 2009; Chiverton et al., 2015), in addition to catchment storage. Figure 2a

174 shows the spatial distribution of BFI across the UK. Higher BFI values are generally found in

175 catchments with greater groundwater influence, such as those in southern and eastern

176 England which are dominated by the UK's Chalk aquifer (Marsh and Hannaford, 2008). Areas
177 of moderate BFI can also be found where there are substantial superficial or glacial deposits
178 such as western England, central Wales and eastern Scotland. In this study, BFI has been
179 grouped into "Low" (0 - 0.25), "Medium" (0.25 - 0.5), "High" (0.5 - 0.75) and "Very High" (0.75
180 - 1). Bins at 0.25 intervals have been generated to test the relationship between varying BFI
181 and multi-annual signal presence. While this potentially produces a non-normal distributed
182 categorisation, it is necessary to effectively test a spread of BFI values. This non-normal
183 distribution is mitigated by our chose of significance test described in the methods section.

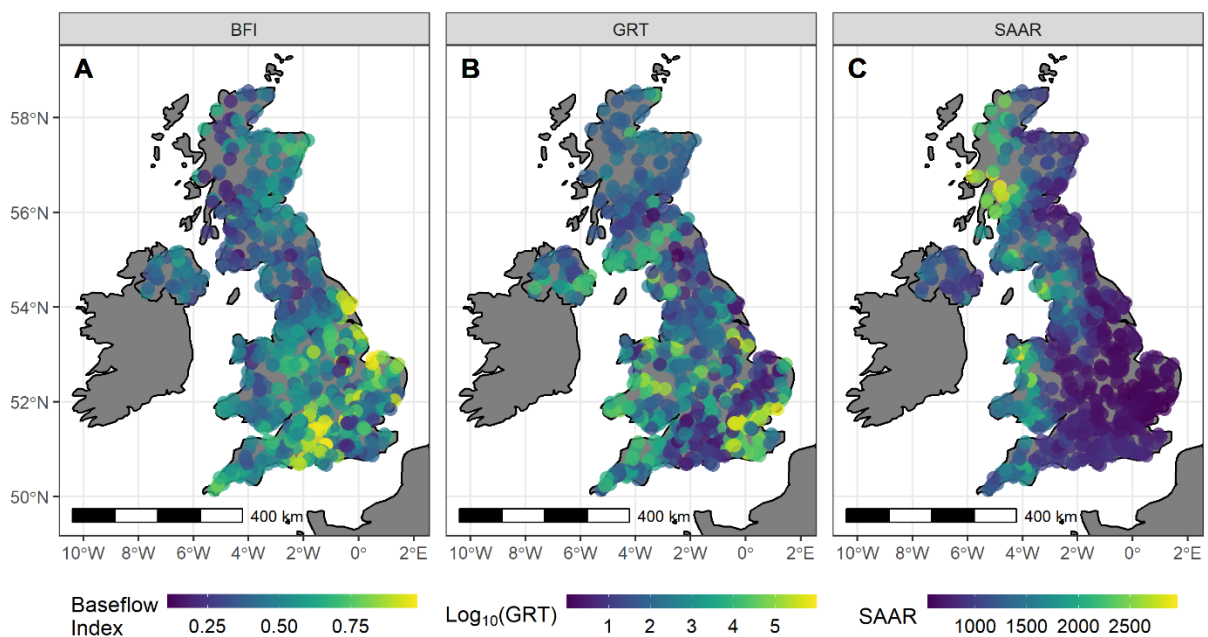
184 In addition to the BFI, the global dataset of Groundwater Response Times (GRT), developed
185 by Cuthbert et al (2019), has been used in this study to estimate the responsiveness of
186 unconfined subsurface pathways. GRT [T] can be conceptualised as a measure of the time
187 required for a groundwater store to return to an equilibrium after a perturbation in recharge,
188 and is given by:

$$\text{GRT} = \frac{L^2 S}{\beta T} \quad (\text{Eq.1})$$

189 where β is a dimensionless constant, T is transmissivity [$L^2 T^{-1}$], S is storativity [-] and L is the
190 characteristic groundwater flow path length approximated for unconfined groundwater
191 systems by the distance between perennial streams [L]. In this study, the mean GRT was
192 taken for each of the NRFA catchments boundaries for each streamflow gauge. Log_{10} of GRT
193 is displayed in Fig. 2b for clarity purposes, as for gauge catchments used in this study the
194 GRT ranges from approximately 1 year to approximately a million years (e.g. in very low
195 permeability geological formations). While the mapping of GRT was carried out using global
196 datasets with their inherent uncertainties, it should nevertheless enable categorisation of the
197 likely timescales of groundwater response sufficiently well for the purposes of this paper. GRT
198 is seen to be lowest (indicating shorter response times) in areas similar to areas of higher BFI;
199 southern and eastern England but excluding the most south-easterly regions which show
200 some of the highest GRT values (indicating longer response times). Lower GRT values are

201 also seen in Northern England. While BFI and GRT appear inversely similar in spatial extent,
 202 their correlation is low ($r = -0.304$). This is to be expected as they measure different aspects
 203 of catchment process. Unlike BFI, which is an empirical measure of the degree to which slower
 204 pathways contribute to streamflow variability (which may encompass groundwater and
 205 throughflow), GRT is an estimate of the responsiveness of groundwater stores. In this study,
 206 GRT is grouped into five categories: 0-4 years 4-8 years; 8-16 years; 16-32 years and greater
 207 than 32 years.

208 Finally, Standard Average Annual Rainfall (SAAR) for the period 1961-1990 is also provided
 209 as metadata in the NFRA. While not used in our analysis, it is provided here to aid later
 210 discussion. There is a clear zonal divide in SAAR distribution in the UK with greater values on
 211 the west coast and lower values found on the east coast of the UK and central England.
 212 Greatest values are found in west Scotland.



213
 214 Figure 2 – Spatial distribution of a. Base Flow Index (BFI), b. Log₁₀(GRT) and c. Standard
 215 Average Annual Rainfall (SAAR) for each streamflow record.

216

217 2.3. Methods

218 2.3.1. Data Pre-processing

219 In this study we follow a similar pre-processing methodology to that set out in Rust et al (2019).
220 The following pre-processing steps were undertaken. Firstly, all time-series were centred on
221 the long-term mean and normalized to the standard deviation to produce a time series of
222 anomalies. This is to allow spectra between rainfall and streamflow (and between sites across
223 the UK) to be directly compared. From these anomalies; three time-series were created for
224 both streamflow and rainfall, namely; monthly, winter-average (DJF) data and summer-
225 average (JJA) data.

226 2.3.2. Continuous Wavelet Transform (CWT) and identification of Multi-annual periodic 227 signals

228 The CWT is a multi-resolution analysis use to quantify the amplitude of periodic components
229 of a timeseries. It has been used increasingly on hydrological datasets to extract information
230 on non-stationary periodic behaviours in rainfall (Rashid et al., 2015), river flow (Su et al.,
231 2017), and groundwater (Holman et al., 2011; Kuss and Gurdak, 2014). We use the package
232 “WaveletComp” produced by Rosch and Schmidbauer (2018) for all transformations in this
233 paper. The wavelet power, W , represents a dimensionless, absolute measure of periodic
234 amplitude at a time index, t , and scale index, s , through a convolution of the data sequence
235 (x_t) with scaled and time-shifted versions of a wavelet:

$$W(\tau, s) = \frac{1}{s} \left| \sum_t x_t \frac{1}{\sqrt{s}} \psi * \left(\frac{t - \tau}{s} \right) \right|^2 \quad (\text{Eq. 2})$$

236 where the asterisk represents the complex conjugate, t is the localized time index, s is the
237 wavelet scale, and dt is increment of time shifting of the wavelet. The choice of the set of
238 scales, s , determines the wavelet coverage of the series in its frequency domain. The Morlet
239 wavelet was favoured over other candidates due to its good definition in both the time and
240 frequency domains (Tremblay et al., 2011; Holman et al., 2011). Since all datasets have been
241 converted to anomalies prior to the CWT, the calculated wavelet power represents the relative
242 strength of periodicities within the frequency spectra of the anomaly dataset. CWT was

243 undertaken on all three dataset time resolutions (monthly, winter-average and summer-
244 average) to gain an understanding of the periodicities within UK seasonal hydrological data.

245

246 2.3.3. Wavelet Significance Testing

247 Environmental datasets generally exhibit non-zero lag-1 autocorrelations (AR1) due to system
248 storages (Meinke et al., 2005). As a result, they can produce low frequencies as a function of
249 internal variance, rather than an external forcing (Allen and Smith, 1996; Meinke et al., 2005;
250 Velasco et al., 2015). In order to assess whether the periodicities detected as part of the CWT
251 are likely to be the result of noise within the dataset, a red-noise (AR1) significance test has
252 been carried out on all wavelet transforms. For this, 1000 randomly constructed synthetic
253 series with the same AR1 as the original time series were created using Monte Carlo methods.
254 Wavelet spectra maxima from these represent periodicity strength that can arise from a purely
255 red noise process. Wavelet powers from the original dataset that are greater than these “red”
256 periodicities are therefore considered to be driven by a process other than red noise, thus
257 rejecting the null hypothesis. It is important to note that this does not test the significance of a
258 relationship with the NAO, but simply the probability that any periodicity detected is the result
259 of internal variance. Teleconnection processes are often noisy meaning identification of
260 significant periodic behaviours in hydrological datasets can be problematic (Rust *et al.*, 2019).
261 While we highlight any periodicities equal to or above a 95 % confidence interval (CI) (≤ 0.05
262 p-values, due to convention), we also report the full range of p-value results in order to accrue
263 an understanding of periodic forcing across the large dataset.

264 2.3.4. Identification of common multi-annual period strengths in rainfall and streamflow

265 An exploratory approach was undertaken to identify the most prominent, common, multi-
266 annual periodicity across the streamflow records. The wavelet powers of defined peaks in the
267 wavelet power spectrum, greater than one year, were identified, since the NAO is expected to
268 produce a dominant, widespread multi-annual periodicity similar to those found in UK

269 groundwater level records (Rust et al, 2019). Where no peak multi-annual periodicity was
270 found (this occurred in 20 datasets; ~3% of the total data); the maximum wavelet power was
271 identified from within the 25th and 75th percentile of the identified peak wavelet powers from
272 the rest of the streamflow dataset. These bounds were used to calculate peak multi-annual
273 periodicities in rainfall datasets, for the winter and summer streamflow time resolutions. In
274 order to isolate the relationship between catchment responsiveness and multi-annual signal
275 strength, the effect of spatially varying signal powers in rainfall needs to be minimised. As such
276 a residual wavelet power was calculated for each of the streamflow gauges, by subtracting
277 the rainfall multi-annual wavelet power from the streamflow multi-annual wavelet power. This
278 is therefore also a measure of how signal strength is modulated between rainfall and
279 streamflow. For the Summer streamflow NAO powers, a pragmatic decision was made to
280 construct the residual using summer streamflow and winter rainfall, given the dominant control
281 of the NAO on winter rainfall totals, the perennial nature of all UK catchments in this study,
282 and the expectation that winter recharge will be a dominant driver for summer baseflow
283 (Hannaford and Harvey, 2010). It is important to note that modulation, in this case, refers to a
284 change in the spectral strength of specific periods between rainfall and streamflow, and not a
285 measure of change in the amplitude of a temporally periodic behaviour between rainfall and
286 streamflow.

287 2.3.5. Testing the relationship between NAO-like signal strength and hydrological 288 pathway characteristics

289 In order to test the significance of the relationship between the BFI and GRT groups and NAO-
290 like signal presence, the Mann Whitney U test (MWU) was undertaken. The MWU tests
291 the null hypothesis that it is equally likely that a randomly selected value from one population
292 will be different to a randomly selected value from a second population. We use this test here
293 to investigate whether populations from each successive pair of ordinal groups (e.g. Low-Med
294 for BFI) have significantly different distributions. The Mann Whitney U test is appropriate for
295 non-normally distributed BFI and GRT datasets.

296 3. Results

297 3.1. Average wavelet power and p-values

298 Wavelet power spectra and p-values for each of the 705 streamflow and catchment rainfall
299 records are displayed in Fig. 3 and 4 respectively. Average wavelet power and p-values across
300 all sites are shown by the thick line in each plot. Wavelet power is a measure of the relative
301 strength of periodic behaviour (periodicity) within a dataset. It should be noted that these
302 spectra are produced from normalised monthly, winter and summer datasets and as such
303 represent signal presence relative to the variance of individual dataset. In the monthly
304 streamflow and rainfall spectra figures, two discrete bands of periodicity can be seen in the
305 average wavelet powers. These are centred on the 1-year and approximately 7-year
306 periodicity; with average 1-year wavelet powers of 0.661 (range: 0.113-0.980) for streamflow
307 and 0.284 (range: 0.051-0.621) for catchment rainfall; and average 7-year wavelet powers of
308 0.056 (range: 0.002-0.360) for streamflow and 0.036 (range: 0.003 and 0.070) for rainfall. The
309 ~7 year periodicity (P7) signal is also exhibited as discrete periodicities in the seasonal data;
310 with mean P7 wavelet powers of 0.274 (0.029 – 0.582) and 0.198 (0.010 – 0.571) for winter
311 and summer streamflow; and 0.253 (0.015 – 0.472) and 0.107 (0.006 – 0.535) for winter and
312 summer catchment rainfall respectively.

313 These strengths are generally reflected in the wavelet p-values, with bands of lower p-values
314 at the 1 and ~7 year in monthly data, and ~7 year in the seasonal data. Wavelet p-values
315 indicate the likelihood that the detected wavelet powers are not the result of external forcing.
316 As such, lower values indicate increased significance of external forcing over the red noise
317 null hypothesis. Wavelet p-values are generally lower in the monthly catchment rainfall spectra
318 (0.002 – 0.996; mean of 0.289), compared with monthly streamflow (0 – 0.995; mean of 0.443),
319 but this may be an artefact of longer autocorrelations in streamflow records relative to rainfall.
320 Wavelet p-values are comparable for the seasonal spectra, with the exception of summer
321 rainfall which shows the lowest significance; (winter rainfall; 0.003 – 0.995 (mean of 0.148);
322 winter streamflow; 0.001 – 0.839 (mean of 0.129); summer rainfall; 0.005 – 0.992 (mean of

323 0.462); summer streamflow; 0.000 – 0.997 (mean of 0.348)). Summer rainfall shows the
324 weakest wavelet powers and greatest p-values for the P7 band.

325

326 Discrete bands of decreased average wavelet p-values can also be seen between 16-32 years
327 for all the streamflow (monthly: 0.502, winter: 0.400, summer: 0.209) and rainfall datasets
328 (monthly: 0.456, winter: 0.569, summer: 0.355). This periodicity band however exhibits
329 negligible average wavelet power indicating minimal influence on variability. In the winter- and
330 summer-average power spectra there is a band of increased strength at the 2-3 year
331 periodicity. In the winter-average data there is no comparably low p-value, suggesting these
332 higher powers are the result of noise within the averaged time series. However, all the summer
333 spectra, appear to exhibit some decreased p-value at this 2-3-year band.

334

335 3.2. Spatial distribution of Wavelet Powers

336 The main multi-annual periodicity detected in the winter and summer river flow data (~7 years)
337 was mapped for seasonal catchment rainfall and streamflow in Fig. 5. The winter spatial
338 distributions show three distinct areas of increased wavelet power and significance, shared
339 between catchment rainfall and streamflow. The largest area is located in the south-west of
340 England and south Wales, extending north into the Midlands and east into the south east of
341 England in the streamflow data. For rainfall, this area encompasses 101 of the 221 catchments
342 with significant (greater than 95% CI) P7 wavelet power, and 224 of the 262 significant sites
343 in streamflow. The two other areas of increased wavelet significance in rainfall and streamflow
344 cover Northern Ireland (20 significant sites for rainfall; 12 for streamflow) and central Scotland
345 (30 significant sites for rainfall; 25 for streamflow). There are also stronger P7 wavelet powers
346 along the west coast of the UK in both winter rainfall and streamflow, however most significant
347 powers (> 95% CI) are found in England and Wales. Additionally, the location of the greatest
348 wavelet powers differs between winter rainfall and streamflow. Winter rainfall shows higher

349 wavelet powers along the south-west peninsula of England, and south Wales, whereas the
350 greatest winter streamflow wavelet powers are found in South and south-eastern England and
351 appear to be co-located over the Chalk and other principal aquifers (Allen et al., 1997).

352 Little spatial structure exists in P7 wavelet power and significance for the summer-average
353 rainfall data. Some increased density in significance is seen towards the south coast of
354 England; however, this may be due to the increased density of sites in this region as seen in
355 Fig. 1, especially given the negligible average P7 wavelet strength displayed in Fig. 3.
356 Conversely, summer-average river flows show some clear spatial structure of wavelet power
357 and significance, in the South of England, where 51 of the 70 sites with significant P7 powers
358 are located. Again, these sites appear to be co-located over the Chalk aquifer (Allen et al.,
359 1997).

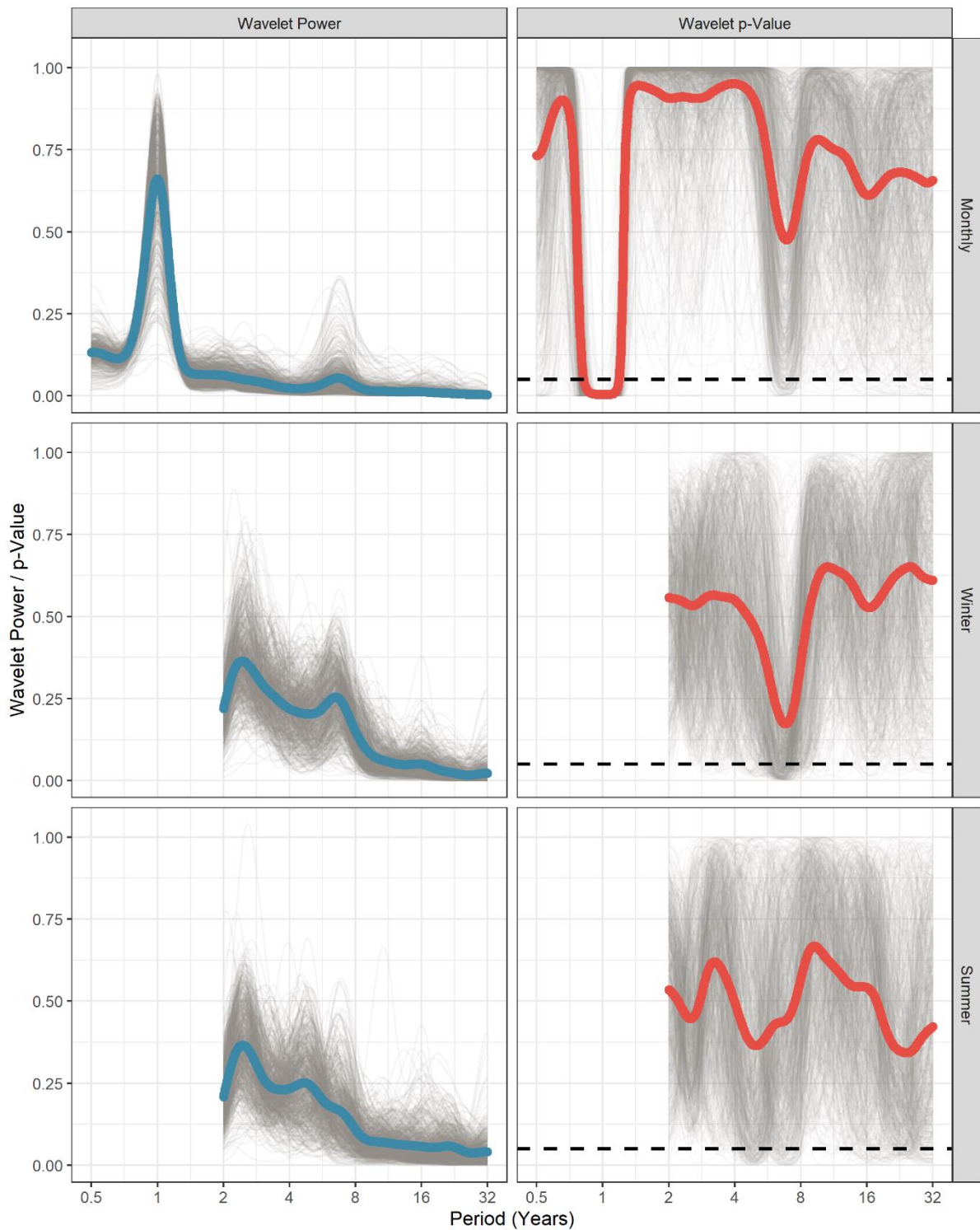
360

361 3.3. Testing of hydrological pathways

362 Figure 6 shows scatter plots of the P7 residual wavelet powers (RWP) for winter and summer
363 streamflow plotted by BFI category (Fig. 6a), and a comparison of median P7 RWP with
364 significance results from the MWU tests (Fig. 6b). Winter P7 median RWPs show a trend of
365 increasing wavelet powers with increasing BFI category, with the exception of between the
366 Low and Medium categories (0.001, -0.002, 0.019 and 0.093 for Low, Medium, High and Very
367 High groups respectively). A similar relationship is seen in the Summer median P7 RWPs (-
368 0.063, -0.079, -0.054 for Low, Medium and High groups), with a notably steeper increase for
369 the final group when compared to winter P7 residuals (increasing to 0.101). This brings the
370 median P7 residual powers for summer streamflow to a comparable magnitude to winter
371 streamflow. In general, winter median P7 residual powers are close to zero except for the Very
372 High category, indicating minimal modulation of P7 signal strength between rainfall and
373 streamflow in the catchments with Low to High BFI. Summer P7 residuals are negative for
374 Low – High BFI catchments indicating a reduction in P7 wavelet powers in streamflow

375 compared to winter rainfall. The median P7 residual for sites in the Very High BFI is the only
376 positive residual for summer streamflow, indicating an increase in relative P7 signal strength
377 between winter rainfall and summer streamflow for these sites.

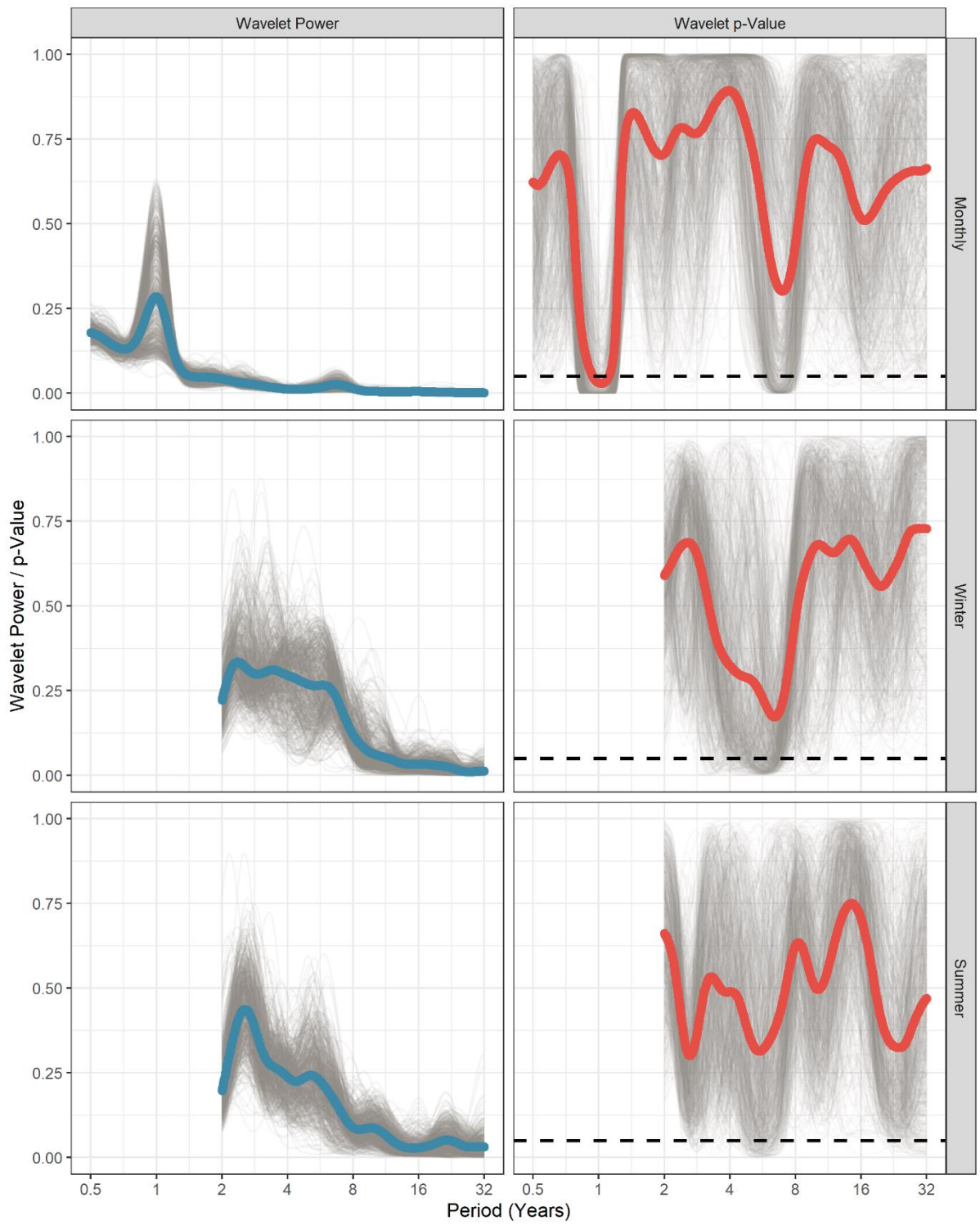
378 Figure 7 shows P7 RWP plotted against Groundwater Response Times (GRT) groups showing
379 all gauges (Fig. 7a), and median RWP with significant results from the MWU tests (Fig. 7b).
380 Winter streamflow shows higher, positive median RWP across all GRT groups (0.056, 0.079,
381 0.017, 0.009, 0.002, for the 0-4, 4-8, 8-16, 16-32 and 32+ year groups respectively), whereas
382 summer streamflow only shows positive RWPs for catchments in the 0-4 and 4-8 year GRT
383 groups (median RWP of 0.014 and 0.024 respectively). GRTs groups greater than or equal to
384 8 years all show negative median RWPs (-0.011, -0.058 and -0.074 for 8-16, 18-32 and 32+
385 year groups respectively). Both winter and summer streamflow show decreasing median
386 RWPs with increasing GRT, with the exception of the 4-8 year GRT group, which shows the
387 greatest median RWP in both winter and summer. Significant difference between GRT groups
388 are found between 0-4 and 4-8, and 4-8 and 8-16 for winter streamflow, and between 4-8 and
389 8-16 for summer streamflow.



390

391 Figure 3 - Stacked streamflow wavelet spectra power (left) and p-values (right) from
 392 normalised Monthly, Winter and Summer resolution data of 705 catchments. 95% Confidence
 393 interval is shown as a dashed black line on the right column figures. Opacity of each average
 394 spectra line has been lowered to allow general trends to be identified.

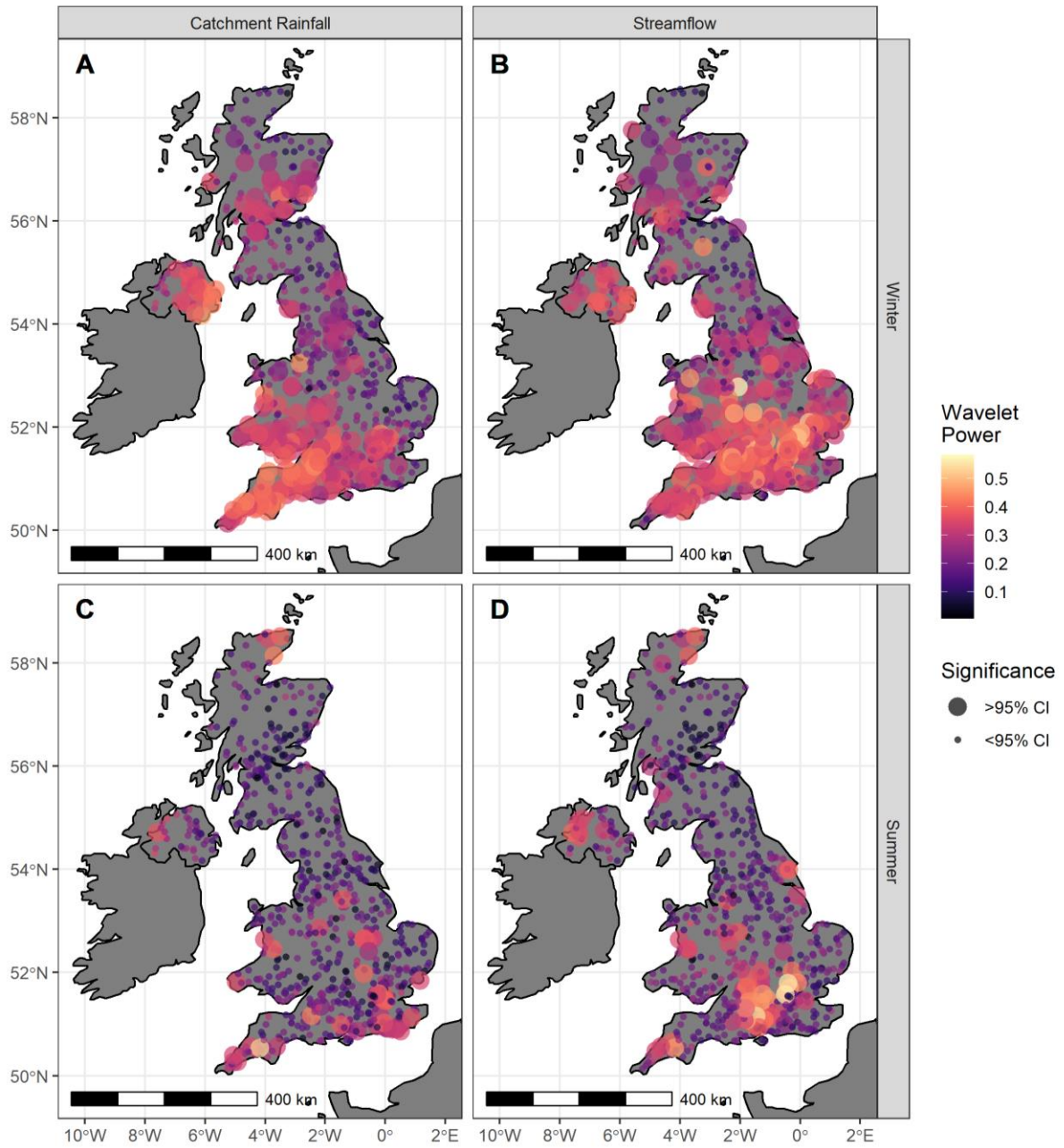
395



396

397 Figure 4 – As Fig. 3 but for catchment rainfall data.

398



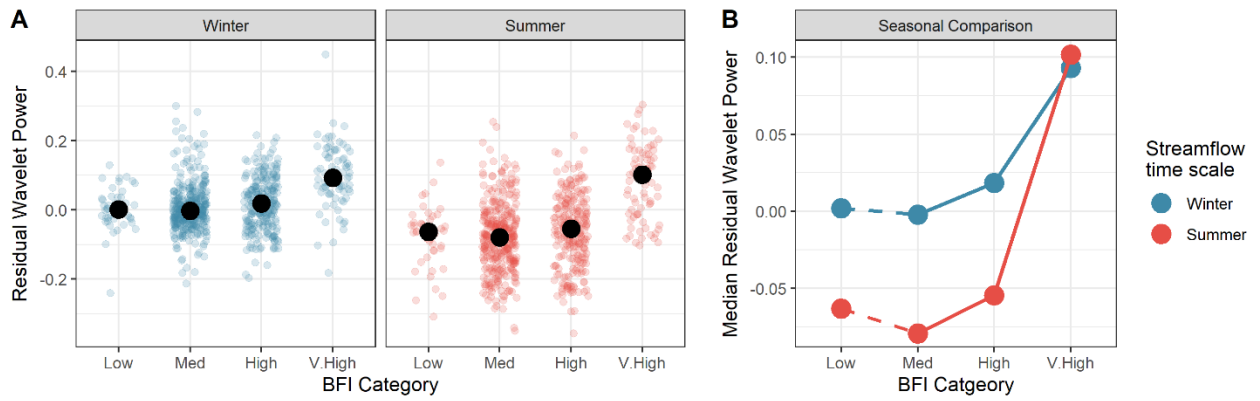
399

400 Figure 5 – Spatial distribution of ~7-year periodicity wavelet power and significance in
 401 catchment rainfall and streamflow, for winter and summer-averaged datasets.

402

403

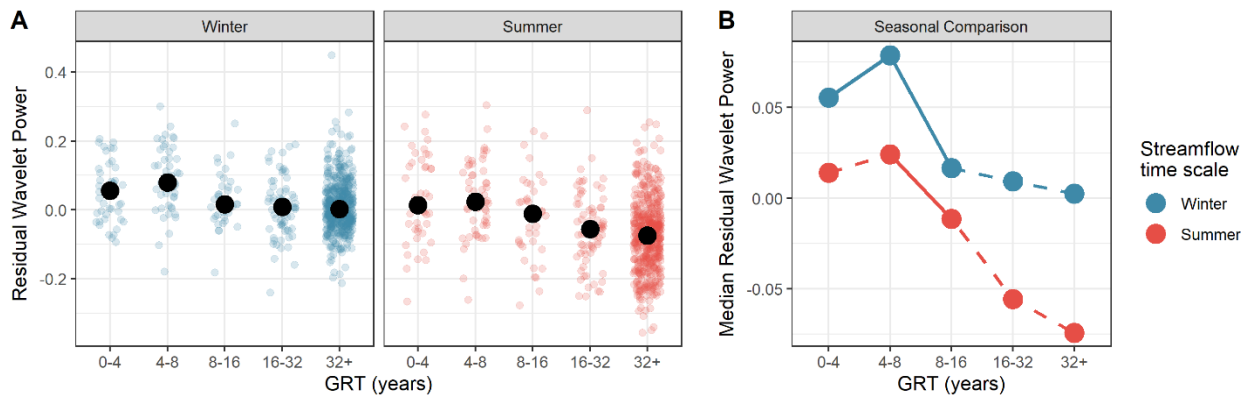
404



405

406 Figure 6 – A) shows jittered scatter plots for residual wavelet powers in winter and summer,
 407 categorised by BFI; bold black points mark the average residual wavelet power for each BFI
 408 category. B) compares these median residual wavelet powers with significant changes
 409 between groups shown as solid lines, and non-significant changes between groups is
 410 shown as dashed lines.

411



412

413 Figure 7 – as figure 6 but for the Groundwater Response Times (GRT)

414

415

416

417

418

419

420

421

422

423

424

425

426 4. Discussion

427 4.1. Detecting a teleconnection between the NAO and UK Streamflow

428 Our results indicate that the dominant common multi-annual periodicity in UK streamflow (and
429 catchment rainfall) is that of an approximately 7-year cycle. This can be seen most clearly in
430 the monthly and winter streamflow spectra (Fig 3; top and middle panel). This cycle compares
431 to the 6- to-9-year pseudo-periodicity documented in the strength of the NAO's atmospheric
432 dipole, which has been associated with multi-annual periodicities in hydrometeorological
433 records globally (Labat, 2010; Rust et al 2019; Tremblay et al., 2011; Kuss and Gurdak, 2014;
434 Holman et al., 2011; Neves et al., 2019). We show here that this ~7 year cycle is wide-spread
435 within rainfall and streamflow variability across the UK, with the majority of streamflow and
436 rainfall records assessed here exhibiting a coherent band of increased periodicity strength and
437 significance around this 7-year frequency range. This, combined with greater significance for
438 this periodicity, and the wide spatial domain on which they are detected, indicates an external
439 control on this multi-annual mode of variability. As such, we build upon evidence in existing
440 research that documents the teleconnection between the NAO and rainfall in Europe and show
441 new evidence of the propagation of the NAO's ~7 year cycle to UK streamflow variability.
442 Additionally, we detect expected differences between signal presence in summer and winter
443 rainfall, showing increased strength and spatial structure of NAO-like signals during the winter
444 months, and weaker summer values with little spatial structure (suggesting noise). This
445 generally agrees with existing research showing that NAO's control over European rainfall is
446 primarily expressed in winter months (Trigo et al., 2004; West et al., 2019). However, it should
447 also be noted that there are multiple interacting climate systems that affect European weather
448 (for instance, the East Atlantic and Scandinavia patterns (Bru and McDermott, 2014) that,
449 while generally weaker than the NAO's influence in European weather variability, may have
450 additional or compounding influence on the cycles detected in streamflow and rainfall
451 presented here. For the remainder of the paper, we will continue to refer to these cycles as

452 NAO-like however, given the NAO's established dominant control on European weather
453 variability (Hurrell and Van Loon; 1997).

454

455 4.2. Controls on multi-annual signals in catchment rainfall

456 We provide new evidence that NAO-like multi-annual periodicities in UK rainfall are seen in
457 the winter months, and are heavily localised to the Southwest of England, South Wales, the
458 east coast of Northern Ireland and central band Scotland (Fig. 5). This is contrary to previous
459 research that has typically found strongest relationships between the NAOI and UK rainfall
460 along the west coast of the UK, particularly the west coast of Scotland (Murphy and
461 Washington, 2001; Fowler and Kilsby, 2002; West et al., 2019). Rust et al. (2018), suggests
462 that the NAO may have two pathways for its modulation on UK rainfall; a fine-scale (e.g. sub
463 annual or annual) atmospheric pathway via modulation of westerly storm tracks (Trigo et al,
464 2002; Parker et al, 2019; Woollings and Blackburn; 2012), and an oceanic pathway via long-
465 term influence on the Gulf Stream (Taylor and Stephens, 1998; Chaudhuri et al., 2011; Watelet
466 et al., 2017). As such, we may expect teleconnection studies that assess the annual
467 relationship between the NAO and rainfall (such as existing research) to better capture the
468 atmospheric pathway. Conversely, studies that assess a longer-term influence (such as the
469 wavelet analysis used here), may better capture the oceanic pathway for NAO control on
470 rainfall (i.e. via the Gulf Stream). Haarsma et al (2015) shows that precipitation in the South
471 West of England exhibits the strongest negative correlation in the UK (~ -0.4) with modelled
472 variability in the Atlantic Meridional Overturning Current (of which the Gulf Stream is part). As
473 such, the increased strength in NAO-like signals in winter rainfall shown here in the South
474 East of England could be explained by the NAO's long-term control on the Gulf Stream.

475

476 4.3. Hydrological drivers for signal strengths

477 We have shown that NAO-like periodicities are localised to specific regions in the UK in winter
478 rainfall (Fig. 5a) and are negligible in summer rainfall (Fig. 5c). This suggests that NAO-like
479 periodicities in summer streamflow do not originate from summer rainfall, and that catchment
480 processes that drive winter rainfall signal propagation to summer streamflow (e.g. subsurface
481 pathways (Haslinger *et al.*, 2014; Folland *et al.*, 2015; Barker *et al.*, 2016)) may inform our
482 understanding of catchment controls on the NAO teleconnection with streamflow. Here, we
483 provide statistically significant evidence that multi-annual periodic signals in rainfall are
484 propagated to streamflow differently between winter and summer months, depending on the
485 contribution from different hydrological pathways (and their response times). Furthermore, we
486 provide evidence that pathways of specific response times propagate these periodic signals
487 to UK streamflow more effectively than others, highlighting the catchment properties that may
488 produce a sensitivity to the NAO teleconnection with streamflow. Below, we discuss how these
489 relationships align with current hydrological understanding.

490 Rust *et al.* (2019) establishes that multi-annual NAO-like periodicities in groundwater level
491 records are considerably stronger than those in co-located rainfall records. Groundwater
492 behaviour generally exhibits longer autocorrelations than rainfall with negligible fine-scale
493 variability (noise), due to the damping effect of subsurface hydrological pathways (Townley,
494 1995; Dickinson, 2004; Gnann *et al.*, 2019). As such, groundwater can express a greater
495 signal-to-noise ratio for low frequency variations (such as those produced by the NAO
496 teleconnection) (Holman *et al.*, 2009; Rust *et al.*, 2018). By comparison, rainfall (which
497 generally contains more fine-scale (hourly – daily) variability), exhibits a lower signal-to-noise
498 ratio which suppresses the proportional strength of multi-annual NAO-like signals (Meinke *et*
499 *al.*, 2005; Brown, 2018). A parallel can be drawn here with hydrological pathway influence on
500 streamflow, as surface pathways more closely reflect rainfall variability and subsurface
501 pathways more closely reflect groundwater variability (Ockenden and Chappell, 2011;
502 Kamruzzaman *et al.*, 2014; Mathias *et al.*, 2016; Gnann *et al.*, 2019).

503 Streamflow driven primarily by surface processes (e.g. BFI < 0.5) exhibits close-to-zero
504 median RWP in winter (Fig. 6b), indicating surface pathways affect minimal modulation of
505 NAO periodicity strength from winter rainfall to winter streamflow; likely due to their relatively
506 short response times (minutes to days) (Mathias *et al.*, 2016). This also explains why the
507 spatial footprint of NAO-like periodicities in winter streamflow (Fig. 5b) generally matches that
508 of winter rainfall (Fig. 5a) as a greater proportion of surface pathway are active in response to
509 greater in-season rainfall (due to more infiltration- or saturation-excess runoff from the land
510 surface) (Ledingham *et al.*, 2019). Summer streamflow, where driven by surface pathways,
511 show minimal sensitivity to NAO periodicities in winter rainfall (negative median RWPs), due
512 to fewer catchment storage mechanisms available convey winter rainfall signals to summer
513 streamflow (Barker *et al.*, 2016), and the weaker of NAO teleconnection with UK summer
514 rainfall (as noted by Alexander *et al.*, (2005); Hurrell and Deser, (2010); West *et al.*, (2019),
515 and indicated here). Conversely, streamflow that is dominated by subsurface pathway
516 influence (e.g. BFI > 0.75) exhibits the greatest NAO periodicities (Fig. 6b). We also see
517 significant increases in NAO periodicity strength with increasing BFI in all but between the
518 lowest two BFI categories (Low – Med). We therefore confirm our expectation that NAO
519 periodicities in groundwater are propagated to streamflow via subsurface pathways. This
520 relationship is also seen in the spatial footprints of NAO periodicities in winter (Fig. 5b) and
521 summer streamflow (Fig. 5d). Gauges with the strongest NAO-like periods in summer and
522 winter streamflow are found in catchments that are within, or that drain, the Chalk outcrop in
523 south central England. These catchments are known to be heavily driven by groundwater
524 behaviour (Marsh and Hannaford, 2008). In Fig. 5b we see the spatial footprint of NAO
525 periodicities in summer streamflow is localised to these Chalk-dominated catchments.
526 Permeable catchments such as those on the Chalk aquifer are known to slowly respond to
527 winter rainfall at a seasonal timescale (Hellwig and Stahl, 2018). As such, these catchments
528 have sufficient subsurface pathway contribution to protract NAO periodicities in winter rainfall
529 through to summer streamflow. Conversely, Fig. 5 also show some areas of the Chalk with
530 relatively low NAO-like periods, such as the southern coast of England. Similarities can be

531 seen here with Marchant and Bloomfield (2018) who identify discrete regions of groundwater
532 level behaviour within the chalk aquifer, with varying autocorrelations. The Chalk of the south
533 coast of England tend to have thinner superficial deposits and negligible glacial deposits
534 (unlike those in the area of the Chalk outcrop), producing a faster recharge response to rainfall
535 with shorter autocorrelations (Marsh and Hannaford, 2008; Marchant and Bloomfield, 2018).
536 Dickinson *et al.*, (2014) highlights the importance of unsaturated zone thickness in modulating
537 periodic signal progression, which may explain why catchments in the southern Chalk exhibit
538 lower signal-to-noise ratios for NAO periodicities.

539 While the relationship between NAO periodicities and streamflow BFI indicates the importance
540 of subsurface pathway contribution to teleconnection strength, properties of the subsurface
541 pathways themselves are expected to modulate periodic signal propagation from rainfall to
542 streamflow (Rust *et al.*, 2018). We show streamflow in catchments with shorter Groundwater
543 Response Times (GRT) exhibit stronger NAO-like periodicities, but the strongest NAO
544 periodicity is found in catchments with GRTs between 4 and 8 years. Townley (1995) shows
545 that where the groundwater response time of a subsurface store is longer than a periodicity in
546 recharge, the system will exhibit larger periodic variations in groundwater head but greater
547 attenuation of periodic discharges at a streamflow boundary. This is because the pathway
548 cannot equilibrate the periodic recharge to its hydraulic boundaries at a sufficient rate.
549 Conversely, where the pathway response time is shorter than that of a periodicity in recharge,
550 groundwater discharge will show greater periodic variations as the entire pathway is able to
551 convey this signal. This may explain the reduction in NAO periodicities seen as GRT increases
552 in Fig. 6b. Where subsurface pathway response times are longer than the principal ~7 year
553 periodicity of the NAO, we may expect the pathway to dampen the signal propagation to
554 baseflow (Townley, 1995; Dickinson, 2004). However, this process fails to explain the reduced
555 NAO periodicity strength seen in our results where GRT is less than the ~7 year NAO
556 periodicity (seen principally in the winter streamflow data). As suggested by Najafi *et al.*,
557 (2017) and Wilby, (2006), faster pathways can exhibit a weaker signal-to-noise ratio, when

558 compared to slower pathways which are known to smooth signal propagation (Barker *et al.*,
559 2016). As such, streamflow in catchments with the shortest GRT (i.e. 0-4 years) may exhibit
560 greater response to finer scale variability in rainfall which supresses the relative strength of
561 the NAO periodicity. This would also explain why summer streamflow does not show a
562 similarly reduced NAO-like period strength for the 0-4 years GRT band, as summer streamflow
563 generally would be expected to exhibit greater signal-to-noise ratios due to a greater
564 proportion of slow pathway contribution. As such, our results suggest that, in addition to the
565 described periodic signal modulations in Townley *et al* (1995), there is an ideal range of
566 subsurface pathway response times that are long enough to produce a greater signal-to-noise
567 ratio, but sufficiently short that there is minimal damping.

568

569 These results may have important implications for streamflow management, as we show that
570 readily available estimates of BFI and GRT may be used to screen or identify catchments
571 where further work may be necessary to understand long-term cyclical behaviour in
572 streamflow. This may be particularly important in ensuring sustainable ongoing use of water
573 resources, such as abstraction for water supply and ecosystem management. This is
574 particularly important for summer streamflow where streamflow services are often vulnerable
575 to drought conditions (Visser *et al.*, 2019). Furthermore, there is a need for consideration of
576 these cycles within water management policy and practice in the UK. For instance, stochastic
577 or probabilistic approaches often used for water resource planning periods may need to be
578 augmented in order to account for the cyclical, non-stationary variability reported here, and for
579 their potential benefits to be realised.

580

581

582 4. Conclusions

583 This paper assesses the degree to which the principal multi-annual periodicity (~7 years) of
584 the NAO is present in streamflow and catchment rainfall records using the Continuous wavelet
585 transform to identify multi-annual periodicities. We provide new evidence for the role of
586 oceanic and atmospheric pathways in propagating NAO periodicities to catchment rainfall, by
587 identifying spatial patterns of statistically significant NAO-like periodicities in UK catchment
588 rainfall and streamflow. This may help further explicate the varying spatial extent of the NAO
589 influence over Europe and the North Atlantic Region. Furthermore, we identify specific
590 streamflow catchment characteristics that are most responsive to the NAO periodicities in
591 catchment rainfall. We find that streamflow that is driven predominantly by subsurface pathway
592 contributions often exhibit greater NAO-like periodicities, and that subsurface pathways with
593 response times comparable in length to the ~7 year periodicity of the NAO produce the
594 greatest sensitivity to the NAO teleconnection. These findings build on the fundamental
595 understanding of periodic signal propagation through hydrological pathways and can aid in
596 the identification of catchments with sensitivities to multi-annual control, for instance those
597 found in climatic teleconnections. The ability to screen catchments for their potential
598 teleconnection-driven multi-annual variability may have direct implications for water
599 management decision making. For example, the permitting of surface water abstractions and
600 their implications for ecologically sensitive streamflow systems. Such information may help to
601 protect vulnerable habitats or aid appropriate investment in surface water abstraction
602 infrastructure. Our results here make necessary steps towards a greater understanding of how
603 climatic teleconnections can be used to improve water resource management practices.

604

605

606

607

608

609 **Data availability.**

610 The streamflow and precipitation data as well as the metadata used in this study are freely
611 available at the NRFA website (<http://nrfa.ceh.ac.uk/>).

612

613 **Author contributions.**

614 WR designed the methodology and carried them out with supervision from all co-authors. WR
615 prepared the article with contributions from all co-authors.

616

617 **Competing interests.**

618 The authors declare that they have no conflict of interest.

619

620 **Acknowledgements.**

621 This work was supported by the Natural Environment Research Council (grant numbers
622 NE/M009009/1 and NE/L010070/1) and the British Geological Survey (Natural Environment
623 Research Council). JB publishes with the permission of the Executive Director, British
624 Geological Survey (NERC). MOC gratefully acknowledges funding for an Independent
625 Research Fellowship from the UK Natural Environment Research Council (NE/P017819/1).

626 We thank Angi Rosch and Harald Schmidbauer for making their wavelet package
627 “WaveletComp” freely available. This study was a re-analysis of existing data that are publicly
628 available from the NRFA at <https://nrfa.ceh.ac.uk/>.

629

630 **Financial support.**

631 This research has been supported by the Natural Environment Research Council (grant nos.
632 NE/M009009/1 and NE/L010070/1), and MOC has been supported by an Independent
633 Research Fellowship from the UK Natural Environment Research Council (NE/P017819/1).

634

635 **References**

636 Acreman, M. C. and Dunbar, M. J.: Defining environmental river flow requirements – a
637 review, *Hydrology and Earth System Sciences*, 8, 861–876. [https://doi.org/10.5194/hess-8-](https://doi.org/10.5194/hess-8-861-2004)
638 861-2004, 2004.

639 Alexander, L. V., Tett, S. F. B. and Jonsson, T.: Recent observed changes in severe storms
640 over the United Kingdom and Iceland, *Geophysical Research Letters*, 32, 1–4.
641 <https://doi.org/10.1029/2005GL022371>, 2005.

642 Allen, M R. and Smith, L A., Monte Carlo SSA: Detecting Irregular Oscillations in the
643 Presence of Colored Noise. *Journal of Climate* 9 (12): 3373–3404.
644 [https://doi.org/10.1175/1520-0442\(1996\)009<3373:MCSPIO>2.0.CO;2](https://doi.org/10.1175/1520-0442(1996)009<3373:MCSPIO>2.0.CO;2). 1996.

645 Barker, L. J., Hannaford, J., Chiveron, A. and Svensson, C.: From meteorological to
646 hydrological drought using standardised indicators, *Hydrology and Earth System Sciences*,
647 20, 2483–2505. <https://doi.org/10.5194/hess-20-2483-2016>, 2016.

648 Bloomfield, J. P., Allen, D. J. and Griffiths, K. J.: Examining geological controls on baseflow
649 index (BFI) using regression analysis: An illustration from the Thames Basin, UK, *Journal of*
650 *Hydrology*. Elsevier B.V., 373, 164–176. <https://doi.org/10.1016/j.jhydrol.2009.04.025>, 2009.

651 Bloomfield, J. P., and B. P. Marchant. Analysis of Groundwater Drought Building on the
652 Standardised Precipitation Index Approach. *Hydrology and Earth System Sciences* 17:
653 4769–87. <https://doi.org/10.5194/hess-17-4769-2013> . 2013.

654 Bouwer, L. M., Vermaat, J. E. and Aerts, J. C. J. H.: Winter atmospheric circulation and river
655 discharge in northwest Europe, *Geophysical Research Letters*, 33, L06403.

656 <https://doi.org/10.1029/2005GL025548>, 2006.

657 Bracken, L. J., Wainwright, J., Ali, G. A., Tetzlaff, D., Smith, M. W., Reaney, S. M. and Roy,
658 A. G.: Concepts of hydrological connectivity: Research approaches, Pathways and future
659 agendas, *Earth-Science Reviews*. Elsevier B.V., 119, 17–34.
660 <https://doi.org/10.1016/j.earscirev.2013.02.001>, 2013.

661 Brown, S. J.: The drivers of variability in UK extreme rainfall, *International Journal of*
662 *Climatology*, 38, e119–e130. <https://doi.org/10.1002/joc.5356>, 2018.

663 Burt, T. P. and Howden, N. J. K.: North Atlantic Oscillation amplifies orographic precipitation
664 and river flow in upland Britain, *Water Resources Research*, 49.
665 <https://doi.org/10.1002/wrcr.20297>, 2013.

666 Bru, L., and McDermott, F. Impacts of the EA and SCA Patterns on the European Twentieth
667 Century NAO-Winter-Climate Relationships. *Quarterly Journal of the Royal Meteorological*
668 *Society* 140: 354–63. <https://doi.org/10.1002/qj.2158>. 2014.

669 Carr, E. J. and Simpson, M. J.: Accurate and efficient calculation of response times for
670 groundwater flow, *Journal of Hydrology*. Elsevier B.V., 558, 470–481.
671 <https://doi.org/10.1016/j.jhydrol.2017.12.023>, 2018.

672 Chaudhuri, A. H., Gangopadhyay, A. and Bisagni, J. J.: Response of the Gulf Stream
673 transport to characteristic high and low phases of the North Atlantic Oscillation, *Ocean*
674 *Modelling*, 39, 220–232. <https://doi.org/10.1016/j.ocemod.2011.04.005>, 2011.

675 Chiverton, A., Hannaford, J., Holman, I. P., Corstanje, R., Prudhomme, C., Hess, T. M. and
676 Bloomfield, J. P.: Using variograms to detect and attribute hydrological change, *Hydrology*
677 *and Earth System Sciences*, 19, 2395–2408. <https://doi.org/10.5194/hess-19-2395-2015>,
678 2015.

679 Chun, K. P., Wheeler, H. S. and Onof, C. J.: Streamflow estimation for six UK catchments
680 under future climate scenarios, *Hydrology Research*, 40, 96–112.

681 <https://doi.org/10.2166/nh.2009.086>, 2009.

682 Crossman, J., Futter, M. N., Whitehead, P. G., Stainsby, E., Baulch, H. M., Jin, L., Oni, S. K.,
683 Wilby, R. L. and Dillon, P. J.: Flow pathways and nutrient transport mechanisms drive
684 hydrochemical sensitivity to climate change across catchments with different geology and
685 topography, *Hydrology and Earth System Sciences*, 18, 5125–5148.
686 <https://doi.org/10.5194/hess-18-5125-2014>, 2014.

687 Cuthbert, M. O., Gleeson, T., Moosdorf, N., Befus, K. M., Schneider, A., Hartmann, J. and
688 Lehner, B.: Global patterns and dynamics of climate–groundwater interactions, *Nature*
689 *Climate Change*. Nature Publishing Group, 9, 137–141. [https://doi.org/10.1038/s41558-018-](https://doi.org/10.1038/s41558-018-0386-4)
690 [0386-4](https://doi.org/10.1038/s41558-018-0386-4), 2019.

691 Dawson, A., Elliott, L., Noone, S., Hickey, K., Holt, T., Wadhams, P. and Foster, I.: Historical
692 storminess and climate ‘see-saws’ in the North Atlantic region, *Marine Geology*, 210, 247–
693 259. <https://doi.org/10.1016/j.margeo.2004.05.011>, 2004.

694 Dawson, A. G., Hickey, K., Holt, T., Elliott, L., Dawson, S., Foster, I. D. L., Wadhams, P.,
695 Jonsdottir, I., Wilkinson, J., McKenna, J., Davis, N. R. and Smith, D. E.: Complex North
696 Atlantic Oscillation (NAO) Index signal of historic North Atlantic storm-track changes, *The*
697 *Holocene*, 12, 363–369. <https://doi.org/10.1191/0959683602hl552rr>, 2002.

698 Dickinson, J. E.: Inferring time-varying recharge from inverse analysis of long-term water
699 levels, *Water Resources Research*, 40, 1–15. <https://doi.org/10.1029/2003WR002650>, 2004.

700 Dickinson, J. E., Ferré, T. P. A., Bakker, M. and Crompton, B.: A Screening Tool for
701 Delineating Subregions of Steady Recharge within Groundwater Models, *Vadose Zone*
702 *Journal*, 13, 1–15. <https://doi.org/10.2136/vzj2013.10.0184>, 2014.

703 Dixon, H., Hannaford, J., and Fry, M. J. The effective management of national hydrometric
704 data: experiences from the United Kingdom, *Hydrological Sciences Journal*, 58:7, 1383-
705 1399, DOI: 10.1080/02626667.2013.787486. 2013

706 Faust, J. C., Fabian, K., Milzer, G., Giraudeau, J. and Knies, J.: Norwegian fjord sediments
707 reveal NAO related winter temperature and precipitation changes of the past 2800 years,
708 Earth and Planetary Science Letters, 435, 84–93. <https://doi.org/10.1016/j.epsl.2015.12.003>,
709 2016.

710 Folland, C. K., Hannaford, J., Bloomfield, J. P., Kendon, M., Svensson, C., Marchant, B. P.,
711 Prior, J. and Wallace, E.: Multi-annual droughts in the English Lowlands: a review of their
712 characteristics and climate drivers in the winter half-year, Hydrology and Earth System
713 Sciences, 19, 2353–2375. <https://doi.org/10.5194/hess-19-2353-2015>, 2015.

714 Forootan, E., M. Khaki, M. Schumacher, V. Wulfmeyer, N. Mehrnegar, A. I. J. M. van Dijk, L.
715 Brocca, et al. Understanding the Global Hydrological Droughts of 2003–2016 and Their
716 Relationships with Teleconnections. The Science of the Total Environment, September.
717 <https://doi.org/10.1016/J.SCITOTENV.2018.09.231>. 2018.

718 Fowler, H. J. and Kilsby, C. G.: Precipitation and the North Atlantic Oscillation: a study of
719 climatic variability in northern England, International Journal of Climatology, 22, 843–866.
720 <https://doi.org/10.1002/joc.765>, 2002.

721 Frankignoul, C., de Coëtlogon, G., Joyce, T. M. and Dong, S.: Gulf Stream Variability and
722 Ocean–Atmosphere Interactions, Journal of Physical Oceanography, 31, 3516–3529.
723 [https://doi.org/10.1175/1520-0485\(2002\)031<3516:GSVAOA>2.0.CO;2](https://doi.org/10.1175/1520-0485(2002)031<3516:GSVAOA>2.0.CO;2), 2001.

724 Fritier, N., Massei, N., Laignel, B., Durand, A., Dieppois, B. and Deloffre, J.: Links between
725 NAO fluctuations and inter-annual variability of winter-months precipitation in the Seine River
726 watershed (north-western France), Comptes Rendus - Geoscience. Academie des sciences,
727 344, 396–405. <https://doi.org/10.1016/j.crte.2012.07.004>, 2012.

728 Gangopadhyay, A., Chaudhuri, A. H. and Taylor, A. H.: On the nature of temporal variability
729 of the gulf stream path from 75° to 55°W, Earth Interactions, 20. [https://doi.org/10.1175/EI-D-](https://doi.org/10.1175/EI-D-15-0025.1)
730 15-0025.1, 2016.

731 Gericke, O. J. and Smithers, J. C.: Revue des méthodes d'évaluation du temps de réponse
732 d'un bassin versant pour l'estimation du débit de pointe, *Hydrological Sciences Journal*.
733 Taylor & Francis, 59, 1935–1971. <https://doi.org/10.1080/02626667.2013.866712>, 2014.

734 Gnann, S. J., Howden, N. J. K. and Woods, R. A.: Hydrological signatures describing the
735 translation of climate seasonality into streamflow seasonality, *Hydrology and Earth System*
736 *Sciences Discussions*, 1–30. <https://doi.org/10.5194/hess-2019-463>, 2019.

737 Guillod, B. P., Jones, R. G., Dadson, S. J., Coxon, G., Bussi, G., Freer, J., Kay, A. L.,
738 Massey, N. R., Sparrow, S. N., Wallom, D. C. H., Allen, M. R. and Hall, J. W.: A large set of
739 potential past, present and future hydro-meteorological time series for the UK, *Hydrology*
740 *and Earth System Sciences*, 22, 611–634. <https://doi.org/10.5194/hess-22-611-2018>, 2018.

741 Gustard, A., Bullock, A., Dixon, J. M.. *Low flow estimation in the United*
742 *Kingdom*. Wallingford, Institute of Hydrology, 88pp. (IH Report No.108).
743 <http://nora.nerc.ac.uk/id/eprint/6050>. 1992.

744 Haarsma, R. J., Selten, F. M., and Drijfhout, S. S. Decelerating Atlantic Meridional
745 Overturning Circulation Main Cause of Future West European Summer Atmospheric
746 Circulation Changes. *Environmental Research Letters*. [https://doi.org/10.1088/1748-](https://doi.org/10.1088/1748-9326/10/9/094007)
747 [9326/10/9/094007](https://doi.org/10.1088/1748-9326/10/9/094007). 2015.

748 Hannaford, J. and Harvey, C.: UK seasonal river flow variability in near-natural catchments,
749 regional outflows and long hydrometric records, BHS Third International Symposium,
750 *Managing Consequences of a Changing Global Environment*, 1–7, 2010.

751 Haslinger, K., Koffler, D., Schöner, W. and Laaha, G.: Exploring the link between
752 meteorological drought and streamflow: Effects of climate-catchment interaction, *Water*
753 *Resources Research*, 50, 2468–2487. <https://doi.org/10.1002/2013WR015051>, 2014.

754 Heape, R., Hirschi, J. and Sinha, B.: Asymmetric response of European pressure and
755 temperature anomalies to NAO positive and NAO negative winters, *Weather*, 68, 73–80.

756 <https://doi.org/10.1002/wea.2068>, 2013.

757 Hellwig, J. and Stahl, K.: An assessment of trends and potential future changes in
758 groundwater-baseflow drought based on catchment response times, *Hydrology and Earth
759 System Sciences*, 22, 6209–6224. <https://doi.org/10.5194/hess-22-6209-2018>, 2018.

760 Holman, I. P., Rivas-Casado, M., Howden, N. J. K., Bloomfield, J. P. and Williams, A. T.:
761 Linking North Atlantic ocean-atmosphere teleconnection patterns and hydrogeological
762 responses in temperate groundwater systems, *Hydrological Processes*. John Wiley & Sons,
763 Ltd, 23, 3123–3126. <https://doi.org/10.1002/hyp.7466>, 2009.

764 Holman, I., Rivas-Casado, M., Bloomfield, J. P. and Gurdak, J. J.: Identifying non-stationary
765 groundwater level response to North Atlantic ocean-atmosphere teleconnection patterns
766 using wavelet coherence, *Hydrogeology Journal*, 19, 1269–1278.
767 <https://doi.org/10.1007/s10040-011-0755-9>, 2011.

768 Hurrell, J. W.: *Decadal Trends in the North Atlantic Oscillation: Regional Temperature and
769 Precipitation*, 1995.

770 Hurrell, J. W. and Deser, C.: North Atlantic climate variability: The role of the North Atlantic
771 Oscillation, *Journal of Marine Systems*, 79, 231–244.
772 <https://doi.org/10.1016/j.jmarsys.2009.11.002>, 2010.

773 Hurrell, J. W., Kushnir, Y., Ottersen, G. and Visbeck, M.: An Overview of the North Atlantic
774 Oscillation, in *The North Atlantic Oscillation: Climatic Significance and Environmental
775 Impact*. American Geophysical Union, 1–35. <https://doi.org/10.1029/134GM01>, 2003.

776 Hurrell, J. W. and Van Loon, H. Decadal Variations in Climate Associated with the North
777 Atlantic Oscillation. *Climatic Change at High Elevation Sites* 36 (3-4): 301–26.
778 <https://doi.org/10.1023/A:1005314315270>. 1997.

779 Jelena Luković, Branislav Bajat, Dragan Blagojević, M. K.: Spatial pattern of North Atlantic
780 Oscillation impact on rainfall in Serbia, *Spatial Statistics*. Elsevier Ltd.

781 <https://doi.org/10.1016/j.spasta.2015.04.007>, 2014.

782 Kamruzzaman, M., Shahriar, M. S. and Beecham, S.: Assessment of short term rainfall and
783 stream flows in South Australia, *Water (Switzerland)*, 6, 3528–3544.
784 <https://doi.org/10.3390/w6113528>, 2014.

785 Kingston, D. G., Lawler, D. M. and McGregor, G. R.: Linkages between atmospheric
786 circulation, climate and streamflow in the northern North Atlantic: research prospects,
787 *Progress in Physical Geography*, 30, 143–174. <https://doi.org/10.1191/0309133306pp471ra>,
788 2006.

789 Kingston, D. G., Hannah, D. M., Lawler, D. M., and McGregor, G. Regional Classification,
790 Variability, and Trends of Northern North Atlantic River Flow. *Hydrological Processes* 25 (7):
791 1021–33. <https://doi.org/10.1002/hyp.7655>. 2011.

792 Kronholm, S. and Capel, P.: Estimation of time-variable fast flow path
793 chemical concentrations for application in tracer-based hydrograph separation analyses,
794 *Journal of the American Water Resources Association*, 52, 6881–6896.
795 <https://doi.org/10.1002/2016WR018797>, 2016.

796 Kuss, A. M. and Gurdak, J. J.: Groundwater level response in U.S. principal aquifers to
797 ENSO, NAO, PDO, and AMO, *JOURNAL OF HYDROLOGY*, 519, 1939–1952.
798 <https://doi.org/10.1016/j.jhydrol.2014.09.069>, 2014.

799 Labat, D. Cross Wavelet Analyses of Annual Continental Freshwater Discharge and
800 Selected Climate Indices. *Journal of Hydrology* 385 (1-4): 269–78.
801 <https://doi.org/10.1016/j.jhydrol.2010.02.029>. 2010

802 Lane, R. A, Coxon, G., Freer, J. E., Wagener, T., Johnes, P. J., Bloomfield, J. P., Greene,
803 S., MacLeod, C., and Reaney, S. M. Benchmarking the Predictive Capability of Hydrological
804 Models for River Flow and Flood Peak Predictions across over 1000 Catchments in Great
805 Britain. *Hydrology and Earth System Sciences* 23 (10): 4011–32.

806 <https://doi.org/10.5194/hess-23-4011-2019>. 2019.

807 Lawler, D., McGregor, G. and Phillips, I.: Influence of atmospheric circulation changes and
808 regional climate variability on river flow and suspended sediment fluxes in southern Iceland,
809 Geophysical Research Letters. Elsevier B.V., 17, 3195–3223. <https://doi.org/10.1002/hyp>,
810 2011.

811 Ledingham, J., Archer, D., Lewis, E., Fowler, H. and Kilsby, C.: Contrasting seasonality of
812 storm rainfall and flood runoff in the UK and some implications for rainfall-runoff methods of
813 flood estimation, Hydrology Research, 50, 1309–1323. <https://doi.org/10.2166/nh.2019.040>,
814 2019.

815 López-Moreno, J. I., Vicente-Serrano, S. M., Morán-Tejeda, E., Lorenzo-Lacruz, J., Kenawy,
816 a. and Beniston, M.: Effects of the North Atlantic Oscillation (NAO) on combined temperature
817 and precipitation winter modes in the Mediterranean mountains: Observed relationships and
818 projections for the 21st century, Global and Planetary Change. Elsevier B.V., 77, 62–76.
819 <https://doi.org/10.1016/j.gloplacha.2011.03.003>, 2011.

820 Marchant, B. P. and Bloomfield, J. P.: Spatio-temporal modelling of the status of
821 groundwater droughts, Journal of Hydrology. Elsevier, 564, 397–413.
822 <https://doi.org/10.1016/J.JHYDROL.2018.07.009>, 2018.

823 Marsh, T. and Hannaford, J.: *UK Hydrometric Register. Hydrological data UK series*. Centre
824 for Ecology and Hydrology, 2008.

825 Mathias, S. A., McIntyre, N. and Oughton, R. H.: A study of non-linearity in rainfall-runoff
826 response using 120 UK catchments, Journal of Hydrology. Elsevier B.V., 540, 423–436.
827 <https://doi.org/10.1016/j.jhydrol.2016.06.039>, 2016.

828 Meinke, H., deVoil, P., Hammer, G. L., Power, S., Allan, R., Stone, R. C., Folland, C. and
829 Potgieter, A.: Rainfall variability of decadal and longer time scales: Signal or noise?, Journal
830 of Climate, 18, 89–90. <https://doi.org/10.1175/JCLI-3263.1>, 2005.

831 Misumi, R., Bell, V. A. and Moore, R. J.: River flow forecasting using a rainfall disaggregation
832 model incorporating small-scale topographic effects, *Meteorological Applications*, 8, 297–
833 305. <https://doi.org/10.1017/S135048270100305X>, 2001.

834 Murphy, S. J. and Washington, R.: United Kingdom and Ireland precipitation variability and
835 the North Atlantic sea-level pressure field, *International Journal of Climatology*, 21, 939–959.
836 <https://doi.org/10.1002/joc.670>, 2001.

837 Najafi, M. R., Zwiers, F. W. and Gillett, N. P.: Attribution of Observed Streamflow Changes in
838 Key British Columbia Drainage Basins, *Geophysical Research Letters*, 44, 11,012-11,020.
839 <https://doi.org/10.1002/2017GL075016>, 2017.

840 Nathan, R. J. and McMahon, T. A.: Evaluation of automated techniques for base flow and
841 recession analyses, *Water Resources Research*, 26, 1465–1473.
842 <https://doi.org/10.1029/WR026i007p01465>, 1990.

843 Neves, M. C., Jerez, S. and Trigo, R. M.: The response of piezometric levels in Portugal to
844 NAO, EA, and SCAND climate patterns, *Journal of Hydrology*. Elsevier, 568, 1105–1117.
845 <https://doi.org/10.1016/J.JHYDROL.2018.11.054>, 2019.

846 Ockenden, M. C. and Chappell, N. A.: Identification of the dominant runoff pathways from
847 data-based mechanistic modelling of nested catchments in temperate UK, *Journal of*
848 *Hydrology*. Elsevier B.V., 402, 71–79. <https://doi.org/10.1016/j.jhydrol.2011.03.001>, 2011.

849 Olsen, J., Anderson, N. J., and Knudsen, M. F. “Variability of the North Atlantic Oscillation
850 over the Past 5,200 Years.” *Nature Geoscience* 5 (11): 808–12.
851 <https://doi.org/10.1038/ngeo1589>. 2012.

852 Parker, T., Woollings, T., Weisheimer, A., O’Reilly, C., Baker, L., and Shaffrey, L. Seasonal
853 Predictability of the Winter North Atlantic Oscillation from a Jet Stream Perspective.
854 *Geophysical Research Letters* 46 (16): 10159–67. <https://doi.org/10.1029/2019GL084402>.
855 2019.

856 Rashid, M., Beecham, S., and Chowdhury, R. K. Assessment of Trends in Point Rainfall
857 Using Continuous Wavelet Transforms. *Advances in Water Resources*. 82, 1-15.
858 <https://doi.org/10.1016/j.advwatres.2015.04.006>. 2015.

859 Riaz, S. M. F., Iqbal, M. J. and Hameed, S.: Impact of the North Atlantic Oscillation on winter
860 climate of Germany, *Tellus, Series A: Dynamic Meteorology and Oceanography*. Taylor &
861 Francis, 69, 1–10. <https://doi.org/10.1080/16000870.2017.1406263>, 2017.

862 Rousseau-Gueutin, P., Love, A. J., Vasseur, G., Robinson, N. I., Simmons, C. T. and De
863 Marsily, G.: Time to reach near-steady state in large aquifers, *Water Resources Research*,
864 49, 6893–6908. <https://doi.org/10.1002/wrcr.20534>, 2013.

865 Rosch, A. and Schmidbauer, H.: WaveletComp 1.1: a guided tour through the R package,
866 available
867 at: <https://pdfs.semanticscholar.org/3825/de34e8ae27624eece03abf6fbb8fd07c795a.pdf> (last
868 access: 20 January 2021), 2018.

869 Rust, W., Holman, I., Bloomfield, J., Cuthbert, M. and Corstanje, R.: Understanding the
870 potential of climate teleconnections to project future groundwater drought, *Hydrology and
871 Earth System Sciences*, 23, 3233–3245. <https://doi.org/10.5194/hess-23-3233-2019>, 2019.

872 Rust, W., Holman, I., Corstanje, R., Bloomfield, J. and Cuthbert, M.: A conceptual model for
873 climatic teleconnection signal control on groundwater variability in Europe, *Earth-Science
874 Reviews*, 177, 164–174. <https://doi.org/10.1016/j.earscirev.2017.09.017>, 2018.

875 Su, L., Miao, C., Borthwick, A. G. L. and Duan, Q.: Wavelet-based variability of Yellow River
876 discharge at 500-, 100-, and 50-year timescales, *Gondwana Research*, 49, 94–105.
877 <https://doi.org/10.1016/j.gr.2017.05.013>, 2017.

878 Svensson, C., A. Brookshaw, A. A. Scaife, V. A. Bell, J. D. Mackay, C. R. Jackson, J.
879 Hannaford, H. N. Davies, A. Arribas, and S. Stanley. Long-Range Forecasts of UK Winter
880 Hydrology. *Environmental Research Letters*: 10 (6): 064006.

881 9326/10/6/064006. 2015.

882 Tabari, H., Hosseinzadeh Talaei, P., Shifteh Some'e, B. and Willems, P.: Possible
883 influences of North Atlantic Oscillation on winter reference evapotranspiration in Iran, *Global*
884 *and Planetary Change*. Elsevier B.V., 117, 28–39.
885 <https://doi.org/10.1016/j.gloplacha.2014.03.006>, 2014.

886 Tanguy, M.; Dixon, H.; Prosdocimi, I.; Morris, D.G.; Keller, V.D.J. Gridded estimates of daily
887 and monthly areal rainfall for the United Kingdom (1890-2017) [CEH-GEAR]. NERC
888 Environmental Information Data Centre. [https://doi.org/10.5285/ee9ab43d-a4fe-4e73-afd5-](https://doi.org/10.5285/ee9ab43d-a4fe-4e73-afd5-cd4fc4c82556)
889 [cd4fc4c82556](https://doi.org/10.5285/ee9ab43d-a4fe-4e73-afd5-cd4fc4c82556). 2019

890 Taylor, A. H. and Stephens, J. A.: The North Atlantic Oscillation and the latitude of the Gulf
891 Stream, *Tellus, Series A: Dynamic Meteorology and Oceanography*, 50, 134–142.
892 <https://doi.org/10.3402/tellusa.v50i1.14517>, 1998.

893 Townley, L. R.: The response of aquifers to periodic forcing, *Advances in Water Resources*,
894 18, 125–146. [https://doi.org/10.1016/0309-1708\(95\)00008-7](https://doi.org/10.1016/0309-1708(95)00008-7), 1995.

895 Tremblay, L., M. Larocque, F. Anctil, and C. Rivard. Teleconnections and Interannual
896 Variability in Canadian Groundwater Levels. *Journal of Hydrology* 410 (3-4): 178–88.
897 <https://doi.org/10.1016/j.jhydrol.2011.09.013>. 2011.

898 Trigo, R. M., Osborn, T. J. and Corte-real, J. M.: The North Atlantic Oscillation influence on
899 Europe: climate impacts and associated physical mechanisms, *Climate Research*, 20, 9–17.
900 <https://doi.org/10.3354/cr020009>, 2002.

901 Trigo, R. M., Pozo-Vazquez, D., Osborn, T. J., Castro-Diez, Y., Gamiz-Fortis, S. and
902 Esteban-Parra, M. J.: North Atlantic oscillation influence on precipitation, river flow and water
903 resources in the Iberian peninsula, *International Journal of Climatology*, 24, 925–944.
904 <https://doi.org/10.1002/joc.1048>, 2004.

905 Uvo, C. B.: Analysis and regionalization of northern European winter precipitation based on

906 its relationship with the North Atlantic oscillation, *International Journal of Climatology*, 23,
907 1185–1194. <https://doi.org/10.1002/joc.930>, 2003.

908 Van Loon, A. F. *Hydrological Drought Explained*. Wiley Interdisciplinary Reviews: Water 2
909 (4): 359–92. <https://doi.org/10.1002/wat2.1085>. 2015.

910 Velasco, E. M., Gurdak, J. J., Dickinson, J. E, Ferré T. P. A., and Corona, C. R. Interannual
911 to Multidecadal Climate Forcings on Groundwater Resources of the U.S. West Coast.
912 *Journal of Hydrology: Regional Studies*. <https://doi.org/10.1016/j.ejrh.2015.11.018>. 2015.

913 Visser, A., Beevers, L. and Patidar, S.: The impact of climate change on hydroecological
914 response in chalk streams, *Water (Switzerland)*, 11. <https://doi.org/10.3390/w11030596>,
915 2019.

916 Wallace, J. M. and Gutzler, D. S.: Teleconnections in the Geopotential Height Field during
917 the Northern Hemisphere Winter, *Monthly Weather Review*, 784–812.
918 [https://doi.org/10.1175/1520-0493\(1981\)109<0784:TITGHF>2.0.CO;2](https://doi.org/10.1175/1520-0493(1981)109<0784:TITGHF>2.0.CO;2), 1981.

919 Walter, K. and Graf, H.-F.: The North Atlantic variability structure, storm tracks, and
920 precipitation depending on the polar vortex strength, *Atmospheric Chemistry and Physics*, 4,
921 6127–6148. <https://doi.org/10.1680-7324/acp/2005-5-239>, 2005.

922 Watelet, S., Beckers, J. M. and Barth, A.: Reconstruction of the Gulf Stream from 1940 to
923 the present and correlation with the North Atlantic Oscillation, *Journal of Physical*
924 *Oceanography*, 47, 2741–2754. <https://doi.org/10.1175/JPO-D-17-0064.1>, 2017.

925 West, H., Quinn, N. and Horswell, M.: Regional rainfall response to the North Atlantic
926 Oscillation (NAO) across Great Britain, *Hydrology Research*, 50, 1549–1563.
927 <https://doi.org/10.2166/nh.2019.015>, 2019.

928 Wilby, R. L.: When and where might climate change be detectable in UK river flows?,
929 *Geophysical Research Letters*, 33, 1–5. <https://doi.org/10.1029/2006GL027552>, 2006.

930 Woollings, T., and Blackburn, M. The North Atlantic Jet Stream under Climate Change and

931 Its Relation to the NAO and EA Patterns. *Journal of Climate* 25 (3): 886–902.

932 <https://doi.org/10.1175/JCLI-D-11-00087.1>. 2012.

933 Wrzesiński, D. and Paluszkiewicz, R.: Spatial differences in the impact of the North Atlantic

934 Oscillation on the flow of rivers in Europe, *Hydrology Research*, 42, 30–39.

935 <https://doi.org/10.2166/nh.2010.077>, 2011.

936 Zhang, X. J., Jin, L. Y., Chen, C. Z., Guan, D. S. and Li, M. Z.: Interannual and interdecadal

937 variations in the North Atlantic Oscillation spatial shift, *Chinese Science Bulletin*, 56, 2621–

938 2627. <https://doi.org/10.1007/s11434-011-4607-8>, 2011.

939

940